Journal of Paleontology, 90(4), 2016, p. 672–688

0022-3360/16/0088-0906
doi: 10.1017/jpa.2016.53

Journal of
PALEONTOLOGY
A JOURNAL OF THE PALEONTOLOGICAL SOCIETY

Variation on cranidial shape of *Parabolinella argentinensis* Kobayashi (Trilobita, Olenidae) from the Tremadocian of northwestern Argentina: taxonomic implications

Daniela S. Monti,[1] María del Huerto Benítez,[2] and Mariano A. Ramirez[3]

[1]Instituto de Ecología, Genética y Evolución de Buenos Aires, Departamento de Ecología Genética y Evolución, Facultad de ciencias Exactas y Naturales, Universidad de Buenos Aires, Intendente Güiraldes 2160, Ciudad Universitaria, Buenos Aires, C1428EGA, Argentina ⟨danielamonti@ege.fcen.uba.ar⟩
[2]Instituto Superior de Correlación Geológica – Facultad de Ciencias Naturales e Instituto Miguel lillio, Universidad Nacional de Tucumán, Miguel Lillo 205, Tucumán CP4000, Argentina ⟨geohuertos@hotmail.com⟩
[3]Museo Argentino de Ciencias Naturales "Bernardino Rivadavia", División Mastozoología, Av. Angel Gallardo 470, Buenos Aires, C1405DJR, Argentina ⟨ma_ramirezchicco@hotmail.com⟩

Abstract.—The late Cambrian-Early Ordovician sequences of the Cordillera Oriental in northwestern Argentina are extensive and highly fossiliferous. The olenid trilobite *Parabolinella argentinensis* Kobayashi sensu Harrington and Leanza, 1957 was reported from a great number of Tremadocian localities and includes a wide range of morphologies. Based on specimens collected from the type locality (Purmamarca, Jujuy) and the quebrada Moya (Huacalera, Jujuy), as well as on material of the Harrington and Leanza collections in the University of Buenos Aires, classic morphometry and geometric morphometry methods were used to evaluate the variability in the cranidium of *P. argentinensis*. The results obtained from the two methodologies are similar. Both analyses allowed the review of the diagnosis of *P. argentinensis*, and the distinction of two new morphologies: *Parabolinella clarisae* n. sp. and *Parabolinella pompadouris* n. sp. The results show how morphogeometrics distinguishes more clearly the three morphotypes and provides graphical representations of the differences between those groups and how from the representations plus the correlation between classical variables and principal components, new diagnostic characters that distinguish the three morphospecies, can be identified.

Introduction

Parabolinella Brøgger, 1882 (Trilobita, Olenidae) is a cosmopolitan genus of the late Furongian-Tremadocian age. It was originally described by Brøgger (1882) from the Tremadocian of Scandinavia, where it is particularly diverse (Westergård, 1922; Henningsmoen, 1957). At present, the genus is recorded in different localities all over the world (e.g., Robison and Pantoja-Alor, 1968; Pribyl and Vanek, 1980; Ludvigsen, 1982; Owens et al., 1982; Fortey and Owens, 1997; Shaw, 1951; Bao and Jago, 2000; Lu and Lin, 1984; Peng, 1991; Terfelt and Ahlgren, 2009; among others). A complete list of the species of *Parabolinella* was provided by Monti and Confalonieri (2013, table 1).

The Cordillera Oriental of southern Bolivia and northwestern Argentina includes late Cambrian-Early Ordovician successions that are representative of the western margin of Gondwana. The Argentinian sequences belong to the Santa Rosita Formation (Turner, 1960), which is characterized by highly fossiliferous shales and sandstones deposited in tide-dominated estuarine to open marine environments. The trilobites from the Cordillera Oriental were first studied by Kayser (1876, 1897), Keidel (1925), Kobayashi (1936, 1937), Harrington (1937, 1938), and Harrington and Leanza (1957), among others. Three species of *Parabolinella* were described from these outcrops: *P. argentinensis* Kobayashi, 1936; *P. coelatifrons* Harrington and Leanza, 1957; and *P.*? *triarthroides* Harrington, 1938. *P. argentinensis* was named by Kobayashi (1936) from the basal Tremadocian of Purmamarca Jujuy; subsequently, Harrington and Leanza (1957) revised its diagnosis and recognized a variable morphology, citing its presence in a great number of localities of late Cambrian-middle Tremadocian age (*Parabolina frequens argentina*, *Jujuyaspis keideli*, *Kainella meridionalis*, and "*Bienvillia tetragonalis-Conophrys minutula*" zones). However, Waisfeld and Vaccari (2003) noted that *P. argentinensis* sensu Harrington and Leanza (1957) may represent more than a single species.

Geometric morphometry proved to be a useful method to distinguish interspecific disparity from intraspecific variation, leading to more robust species delimitation, diversity estimates, biostratigraphic correlation, and to detect evolutionary patterns in a phylogenetic context (e.g., Hughes, 1994; Hughes and Chapman, 2001; Crônier et al., 2005; Adrain and Westrop, 2006; Webster, 2007, 2009; Hopkins and Webster, 2009; Webster, 2011; Abe and Lieberman, 2012; Gendry et al., 2013). Landmark-based methods allow taxonomists to obtain additional characters of the shape of a particular structure that can help delimit taxa (e.g., Mutanen and Pretorius, 2007). Geometric morphometric approaches offer a powerful tool to depict and statistically quantify differences in form (Webster and Sheets, 2010). However, Zelditch et al., (2004) suggested the possibility of using these methods to detect a mathematically optimal discriminator for different species, but this discriminator might not be biologically useful in making identifications (or diagnoses). Regarding the family Olenidae, Kim et al., (2002, 2009) studied the variation in the morphology of the cranidium of *Triarthrus becki* Green, 1832 and its relation with the size and examined geographic patterns of variation in cranidial shape, providing valuable phylogenetic information.

In the present work, classic morphometry and geometric morphometry (landmark-based methods) were used to evaluate the variability of the cranidium of *P. argentinensis* s. Harrington and Leanza. The diagnosis of this species was emended and its systematics revised. In addition, the diversity and distribution of *Parabolinella* in northwestern Argentina was discussed. Also, in the context of the increasing use of geometric morphometrics in taxonomic and systematic studies, the usefulness of this method to discriminate species was discussed.

Materials and methods

Materials and geological settings.—The studied specimens were collected from two localities with Ordovician outcrops in the Cordillera Oriental Argentina at the quebrada de Humahuaca: the Purmamarca region and the quebrada Moya, Jujuy province. Also, specimens of the "Harrington and Leanza Collection" from the Alfarcito region, Jujuy province and the Iruya region, Bocoyá river and Nazareno river, Salta province were used (Fig. 1).

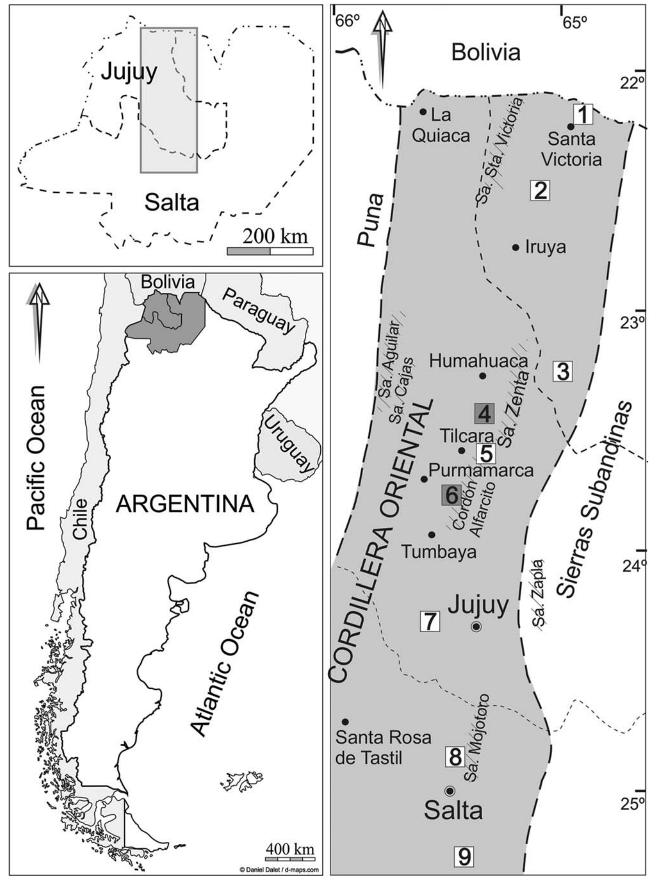

Figure 1. Maps show the location of the Western Cordillera of Argentina. Right: the provenances of the specimens are indicated. **(1)** Santa Victoria region, over 20 km from the city of Santa Victoria and Angosto de Santa, Victoria (22°12'S, 64°52'W). **(2)** Iruya region: Bocoyá river, (upper Iruya river) (22°30'S 65°10'W) and Nazareno river (tributary of Iruya river) (22°41'S, 65°5'W). **(3)** Negrito river (tributary of Santa Cruz river), west of San Antonio de la Nueva Oran city, (23°14'S, 64°29'W). **(4)** Quebrada Moya, eastern margin of the Grande river, 5 km southeast of Uquía (23º19'S, 65º20'W). **(5)** Alfarcito area, eastern side of Quebrada de Humahuaca, 3 km east of Tilcara city (23º34'S, 65º19'W). **(6)** Quebrada Salto Alto, eastern margin of the Grande river (23º45'S, 65º27'W). **(7)** Reyes river, 1 km upstream from the termas de Reyes Hotel, northwest of San Salvador de Jujuy (24°9'S, 65°29'W). **(8)** La Caldera region, western margin of La Caldera river, 15–20 km north of Salta (24°38'S, 65°23'W). **(9)** Cumbre de Castillejo, approximately 25 km south of the city of Salta: quebrada Pinguiyal (25°18'S, 65°28'W) and quebrada Ovejeria (25°18'S, 65°27'W).

The Casa Colorada, Alfarcito, and Rupasca Members (= "Casa Colorada shales," "Alfarcito limestones," and "Rupasca shales" sensu Harrington and Leanza, 1957) of the Santa Rosita Formation are well exposed at quebradas Casa Colorada, San Gregorio and Rupasca, in Alfarcito region (Buatois and Mángano, 2003). These sequences were studied in great detail and abundant paleontological, stratigraphic, and geological information is available (see Harrington and Leanza, 1957; López and Nullo, 1969; Moya, 1988; Zeballo et al., 2003, 2005, 2008, 2011; Buatois et al., 2006; Zeballo and Tortello, 2005; Zeballo and Albanesi, 2013). The studied specimens were collected from the dark shale facies of the upper part of the Rupasca Member (Fig. 2). At the quebrada Salto Alto, Purmamarca region, outcrops the Alfarcito Member (Zeballo and Albanesi, 2009) (= "Purmamarca shales" sensu Harrington and Leanza, 1957). It consists of 35 m of thinly laminated, very disturbed black shale sand few interbedded siltstones which become more frequent towards the upper part of the sequence (Fig. 2). In the shales, an olenid fauna occurs in association with the agnostoids (Kobayashi, 1936; Harrington, 1938; Harrington and Leanza, 1943, 1952, 1957; Aceñolaza and Aceñolaza, 1992; Aceñolaza, 1996; Mángano et al., 1996; Tortello and Aceñolaza, 1999; Aceñolaza et al., 2001). The presence of *Jujuyaspis keideli* in these outcrops indicates a basal Tremadocian age for this unit (Fig. 2); the age is also supported by graptolite faunas (Di Cunzolo and Alfaro, 2008). Seven samples were collected from the pelitic section at Salto Alto (Fig. 2). At the quebrada Moya, the Alfarcito and Rupasca Member are represented mainly by black shales, fine sandstones, and gray-green siltstones (Buatois and Mangano 2003; Buatois et al., 2006, Tortello et al., 2013). The studied specimens come from four samples collected from the dark shale facies of the upper part of the Alfarcito Member, which comprises 35 m of thinly laminated, very disturbed black shales and fine sandstones, with a few interbedded limestone levels (Fig. 2). Both, sandstone and shale bear significant faunas of trilobites, palynomorphs and graptolites, while a diverse fauna of conodonts is found in the sandy levels (Moya, 1988; Aceñolaza and Albanesi, 1997; Di Cunzolo et al., 2003; Rubinstein et al., 2003; Aráoz and Vergel, 2006; Vergel et al., 2007). A low-diversity conodont assemblage of the *Cordylodus angulatus* Zone, and the record of *Rhabdinopora flabelliformis* ssp., indicate an early to middle Tremadocian age (Tortello et al., 2013) (Fig. 2). At the Bocoyá river and the Nazareno river, thinly laminated shales,

https://doi.org/10.1017/jpa.2016.53 Published online by Cambridge University Press

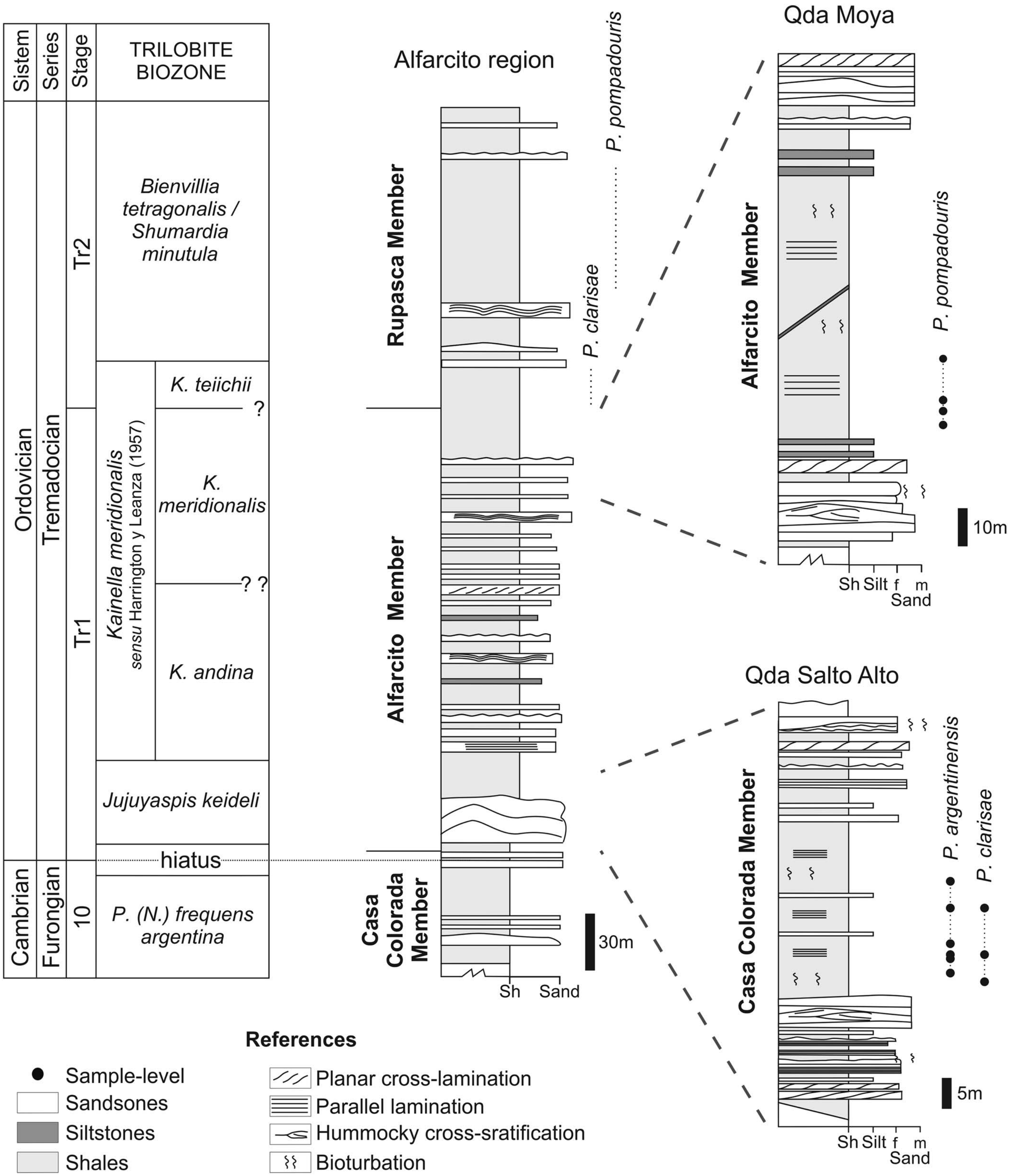

Figure 2. Correlation of the stratigraphic sections at the three localities where specimens were collected. The simplified stratigraphic section of Alfarcito region is based on Zeballo et al. (2003), Zeballo and Tortello (2005), and Zeballo et al. (2005). Left: a scheme of the trilobite biozone is shown (based on the proposal of Vaccari et al. 2010 for the Tremadocian of the Central Andean Basin).

representing the lower Tremadocian of Alfacito Member, are exposed. These dark gray shales bear abundant remains of trilobites of the *Kainella meridionalis* Biozone (Harrington and Leanza, 1957).

In addition, specimens of *Parabolinella* of "Harrington and Leanza Collection" from Tremadocian units exposed on different localities of the Cordillera Oriental were included: Santa Victoria region, Negrito river (tributary of Santa Cruz river), La Caldera region, Reyes river, Cumbre de Castillejo region (Fig. 1). Stratigraphic references published in Harrington and Lenaza (1957) are ambiguous so this material was used as complementary for both description and analysis.

The studied specimens are preserved as internal and external molds, as well as imprints of external molds. A majority of them have suffered minor tectonic distortion. Disarticulated elements of the trilobite exoskeleton prevail, dominated by cranidia. All the specimens included in the analyses are holaspids.

Morphometric analysis.—To quantify the variation of the cranidial shape of *P. argentinensis* s. Harrington and Leanza, two morphometric approaches were used: (1) classical morphometry, and (2) landmark-based geometric morphometry. Measurements of 69 specimens, corresponding to three groups defined by qualitative characters were taken, and ten morphometric variables were determined (Fig. 3.1). Subsequently, seven new variables were generated from the ratios of the original ones (Table 1). To order the specimens according to the morphometric variability observed, a principal component analysis (PCA) from the correlation matrix was performed and a canonical variate analysis (CVA)/MANOVA was performed to test for significant differences among the three groups previously defined, both with PAST 2.15 (Hammer et al., 2001).

For the landmark-based geometric morphometry approach, 63 digital images of the cranidium of the three morphotypes were taken at the same focal distance. In the cases where the cranidium had an incomplete side, the full half was reflected, to include a greater number of specimens. A total of 12 landmarks (type I and II of Bookstein, 1991) and four semi-landmarks (Landmarks type III of Bookstein, 1991, see Bookstein, 1997) were digitalized (Fig. 3.2, Table 2) with tpsDig 2.16 (Rohlf, 2010a). The sliding semi-landmarks criteria used was minimum bending energy (BE; Bookstein, 1996, 1997; Green, 1996; Bookstein et al., 2002), which consist of slide semi-landmark points along the contour to minimize the bending energy necessary to produce the change in the outline relative to the reference form (Bookstein, 1997; Gunz et al., 2005; Pérez et al., 2006). A generalized least-squares Procrustes analysis (GLS, also called a generalized procrustes analysis, GPA, Goodall, 1991; Rohlf, 1999) was performed to estimate a mean shape and to align the specimens. Then, each individual configuration of landmarks of the aligned specimens was compared to the consensus, using the deformation method TPS function, which display directionality and degree of shape change relative to a mean consensus shape. Thus, the partial warp scores (including the non-uniform component and two uniform components) for each individual were obtained, and those were stored in a single matrix, which was the input to a relative warp analysis (RWA). All this was carried out by the program TpsRelW 1.49 (Rohlf, 2010b). To quantify the differences among the three groups previously defined, the partial procrustes

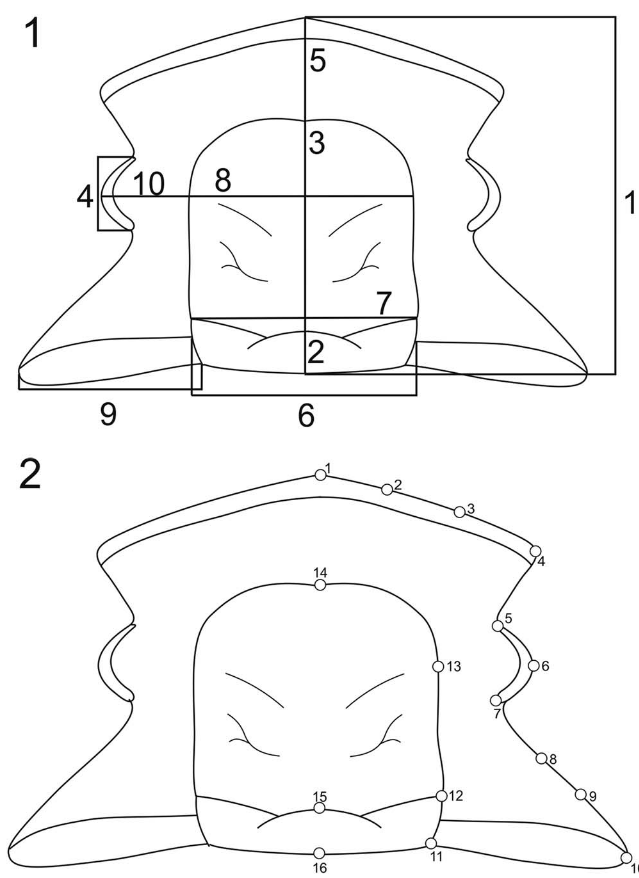

Figure 3. Figure showing the datasets used in the morphometry analyses. **(1)** Measurements used in the classic morphometry analysis. The numbers indicate the variables: (**1.1**) length of the cranidium, (**1.2**) length of the occipital ring, (**1.3**) length of the glabella, (**1.4**) length of the palpebral lobes, (**1.5**) length of the preglabellar field, (**1.6**) width of the occipital ring, (**1.7**) width of the glabella at the base, (**1.8**) width of the glabella at the eye line, (**1.9**) width of the posterior fixigenae, and (**1.10**) width of the interocular genae. **(2)** Landmarks distribution on the cranidium used in the geometric morphometry analysis. The numbers represent the position of the landmark (see Table 2 for description).

Table 1. Description of variables used in the classic morphometry analysis.

Variables	Description
1	Width glabella (base)/length glabella
2	Length palebral lobes/length glabella
3	Width interocular genae/width glebella (eyes)
4	Width posterior fixigenae/width occipital ring
5	Length preglabellar field/length occipital ring
6	Length glabella/length cranidium
7	Length occipital ring/length glabella

Table 2. Description and type of the landmarks used in the geometric morphometry analysis.

Landmark	Description	Type of Homology	
1.	Maximum of curvature anterior of the cranidium	2	
2 ; 3.	Anterior margin of the cranidium	3	*
4.	Anterolateral corners of the cranidium	2	
5.	Most distal anterior point of the papebral lobes	2	
6.	Maximum of curvature (exasag.) of the palpebral lobes	2	
7.	Most posterior point of the palpebral lobes	2	
8 ; 9.	Posterior branch of the facial suture	3	*
10.	Posterolateral corners of the cranidium	2	
11.	Intersection between the posterior margin of the fixigenae and the occipital ring	1	
12.	Intersection between S0 and axial furrows	1	
13.	Axial forrows at eye line	2	
14.	Preglabellar furrow at the sagital plane	1	
15.	S0 at the sagital plane	1	
16.	Posterior margin of the occipital ring at the sagital plane	1	

*Semi-landmarks.

https://doi.org/10.1017/jpa.2016.53 Published online by Cambridge University Press

distance between the consensus configurations of each species was calculated and then the significance of the observed difference between the species means was tested using a bootstrap-based approach utilizing Goodall's F-test (Goodall, 1991; Dryden and Mardia, 1998). The observed F-value is compared to the range of F-values obtained by randomly assigning specimens to samples (1,600 replicates). This was performed using TwoGroup8 software (Sheets, 2014). Details of the methodology used are summarized in Webster and Sheets (2010) and Webster (2011). In addition, a CVA based on procrustes distances was conducted with MorphoJ 1.02E (Klingenberg, 2011). Finally, to recognize variables that can be easily identified as characters in new specimens to separate the three groups, a correlation between the first two axes of the RWA and a series of linear variables (length [L.] preglabellar field/L. occipital ring; width [W.] glabella (base)/L. glabella; L. glabella/L. cranidium W. interocular genae/W. glabella (eyes); W. posterior fixigenae/W. occipital ring; L. occipital ring/L. cranidium L. occipital ring/L. glabella; L. palpebral lobes/L. glabella) was carried out with InfoStat (Di Rienzo et al., 2014).

The relation between shape and size was explored for all the data, and for each group. For this, the centroid size (CS), defined as the square root of the squared distance between each landmark and the centroid of the landmark configurations summed over all landmarks, was calculated for each specimen. This value is an estimator of size that in absence of allometry is independent of the shape. However, when allometry is present, there is a relationship between the CS and any function that express "shape." Thereby, the partial warp scores (calculated as explained above, using as reference form, the consensus of all data and of each group, respectively) were regressed in a multivariate regression against logarithm of the CS (this analysis was performed for all the data and for each group, separately) to evaluated the proportion of shape that was explained by the size. The regression model assumes linearity between shape and size. The residuals of the regression are the deviations of an individual from the mean shape expected for its size. The summed squared residual (SSresidual) can be used to estimate shape deviations not attributable to allometry. The shape changes explained by allometry (SStotal) will be the difference between summed squared total (SStotal) of the sample and the SSresidual. The ratio between SSmodel and SStotal gives the proportion of the total variance explained by allometry. To test significance of the multivariate regression, a permeation test (10,000 replicates of bootstraps resampling) was used. All this was carried out by the program TpsRegr 1.41 (Rohlf, 2011).

Results

Classic morphometry.—The two primary axis of the PCA accounts for 68.324% of the variability (Fig. 4) and differentiate three groups of *Parabolinella argentinensis* sensu Harrington and Leanza. The first axis, which explains 50.605% of the variability, separates the specimens into two groups, one of which is coincident with *P. clarisae* n. sp., whereas the other corresponds to *P. argentinensis* s. s. + *P. pompadouris* n. sp. (Fig. 4). The positive values of this axis correlate with: L. palpebral lobes/L. glabella (0.7584), W. interocular genae/W. glabella (eyes) (0.841), L. preglabellar field/L. occipital ring (0.8599), and W. posterior fixigenae/W. occipital ring (0.8195); and the negative values correlate with: L. glabella/L. cranidium (0.9091) (Fig. 4). The group of *P. clarisae* is located on the negative values of the axis; it is characterized by having relatively small palpebral lobes, interocular genae, preglabellar field and posterior fixigenae, and a relatively long glabella. The second axis explains 17.719% of the variability and separates *P. argentinensis*, on the positive values and *P. pompadouris* on the negative values (Fig. 4). This axis positively correlates with L. occipital ring/L. glabella (0.7364) and W. glabella (base)/L. glabella (0.7137) (Fig. 4). This means that *P. argentinensis*, in contrast to *P. pompadouris*, shows a relatively long occipital ring. The CVA/MANOVA show significant differences between the three groups ($P<0.01$). Hotelling's contrasts indicate that the three groups differ significantly and the cross-classification table shows a global error of 4.35%.

Landmark-based geometric morphometry.—The two primary axes of the RWA account 53.93% of the variability (Fig 5.1). The first axis explains 36.79% of the variability and separates the three defined morphotypes into two groups: *P. argentinensis* s.s. + *P. pompadouris* n. sp., located on the negative region and *P. clarisae* n. sp. placed on the positive region (Fig. 5.1). This axis shows shape variation in the length of the preglabellar field, the angle of divergence of the anterior section of the facial suture, the width of the interocular genae and the relative size of the glabella, with negative score values corresponding to specimens with a more developed preglabelar field, a bigger angle of the anterior branch of facial suture, a wider interocular fixigenae and a smaller glabella (Fig. 5.1). The RW2 explains 17.15% of the total variance and shows variability in the form of the anterior margin, the angle of divergence of the anterior section of the facial suture, the width of the interocular genae, the direction of the posterior facial suture and the development of the posterior fixigenae. The negative values correspond to specimens with an acuminate anterior margin, a less divergent anterior branch of the facial suture, a less developed interocular genae, a narrower posterior fixigenae and a posterior branch of the facial suture more convex and directed posteriorly (Fig. 5.1). Most of the specimens of *P. argentiensis* are located on the positive region while *P. pompadouris*; is placed in the negative region (Fig. 5.1). Finally, the RW3, which explains the 9.88% of the total variability, describes the variation among the width of interocular genae, the length of the preglabellar field and the direction of the anterior branch of the facial suture, with negative score values corresponding to specimens with less divergent anterior branch of the facial suture, a more developed preglabellar field and less developed interocular genae (Fig. 5.2). Two groups of *P. pompadouris* can be recognized in this axis, corresponding to the two localities where this species is found. While those specimens from Bocoyá river lie on the negative values, those from Nazareno river and quebrada Moya are located on the positive values (Fig. 5.2). The paired comparisons of the mean shapes of each species using Goodall's F-test show significant differences in the observed mean shape between all samples (Table 3). Furthermore, the CVA, carried out from the procrustes distances, shows significant differences between the three groups.

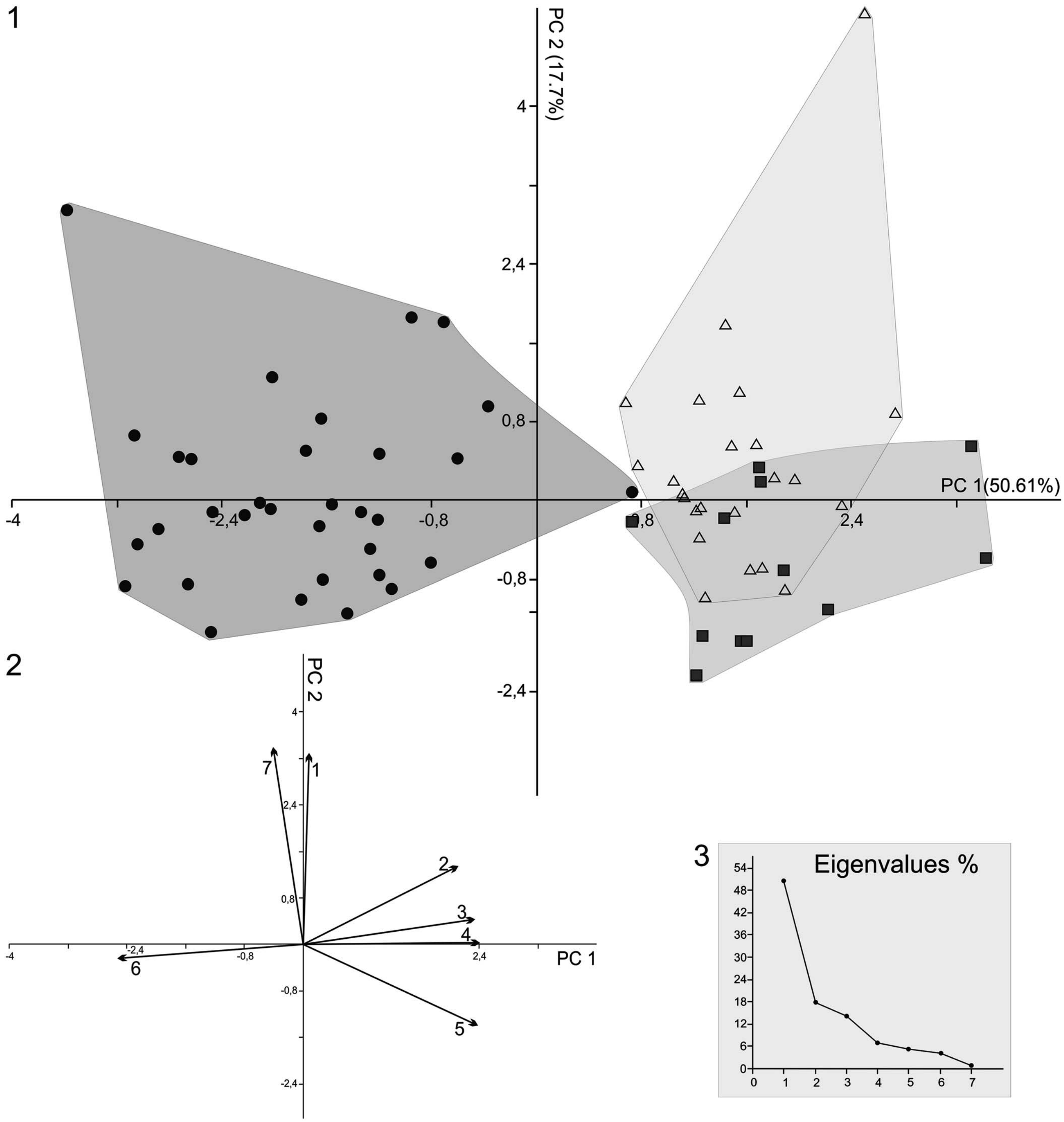

Figure 4. **(1)** Scatterplot of the two first components of the PCA performed with morphometric variables. White triangles: *Parabolinella argentinensis* s. s. Kobayashi. Gray squares: *Parabolinella pompadouris* n. sp. Black circles: *Parabolinella clarisae* n. sp. **(2)** Correlation of the variables with the two first PCs. The numbers indicate the variables. (**2.1**) Width glabella (base)/length glabella. (**2.2**) Length palpebral lobes/length glabella. (**2.3**) Width interocular genae/width glabella (eyes). (**2.4**) Width posterior fixigenae/width occipital ring. (**2.5**) Length preglabellar field/length occipital ring. (**2.6**) Length glabella/length cranidium. (**2.7**) Length occipital ring/length glabella. **(3)** Graphic showing the eigenvalues for each PC.

The RW1 which separates *P. clarisae* from *P. argentinensis* + *P. pompadouris*, negatively correlates with L. preglabellar field/L. occipital ring (r(pearson) $= -0.73$, $P >> 0.05$); W. interocular genae/W. glabella (eyes) (r(pearson) $= -0.74$, $P >> 0.05$); W. posterior fixigenae/W. occipital ring (r(pearson) $= -0.71$, $P >> 0.05$) and L. palpebral lobes/L. glabella (r(pearson) $= -0.59$, $P >> 0.05$); and it positively correlates with L. glabella/L. cranidium (r(pearson) $= 0.85$, $P >> 0.05$). The second axis, which discriminates between *P. argentinensis* and *P. pompadouris*, does not show clear correlations with the classic variables explored (Table 4).

Thereby, *P. argentinensis* is characterized by having a well-developed preglabellar field, a wide interocular genae and a short glabella with narrower, subquadrate base, whereas

https://doi.org/10.1017/jpa.2016.53 Published online by Cambridge University Press

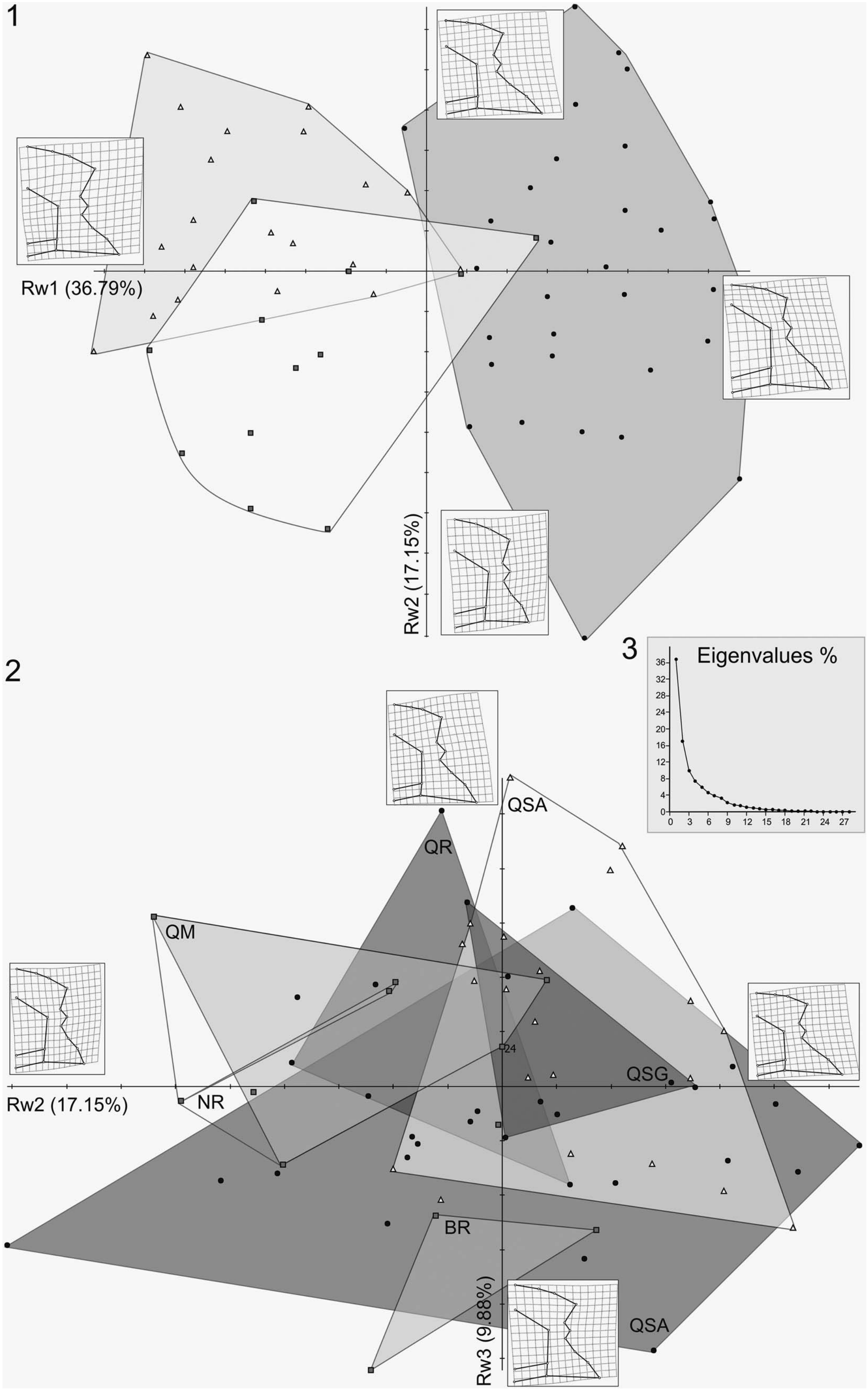

Figure 5. (**1**) Distribution of specimens in the two primary axis of the relative warp analysis. (**2**) Scatterplot of the Rw2 vs Rw3. Thin-plate spline indicates the extreme shape for each axis. White triangles: *Parabolinella argentinensis* s. s. Kobayashi. Gray squares: *Parabolinella pompadouris* n. sp. Black circles: *Parabolinella clarisae* n. sp. Convex hulls indicate the species (**1**) and localities (**2**). (**3**) Graphic showing the eigenvalues for each RW. QSA, Quebrada Salto alto; QSG, Quebrada San Gregorio; QR, Quebrada Rupasca; QM, Quebrada Moya; NR, Nazareno river; BR, Bocoyá river.

https://doi.org/10.1017/jpa.2016.53 Published online by Cambridge University Press

Table 3. Pairwise nonparametric statistical comparisons of the mean cranidial shape between the three species.

Species Comparison	Partial Between means	Procrustes Lower 95% limit	Distance Upper 95% limit	Goodall F	s F-Test *P*
P. argentinensis vs *P. clarisae*	0.0803	0.071	0.0927	20.02	0.0006
P. argentinensis vs *P. pompadouris*	0.0554	0.0492	0.0728	4.99	0.0006
P. pompadouris vs *P. clarisae*	0.0749	0.0602	0.0952	8.23	0.0006

The lower and upper 95% confidence limits and significance value of Goodall's F-test are based on 1,600 bootstraps.

Table 4. Coefficient of Pearson's correlation for each classical variables and principal RWs.

Component	Variable	Pearson Correlation	*P*	
RW1	L. preglabellar field/L. occipital ring	−0.73	0.000	*
RW1	W. glabella (base)/L. glabella	0.05	0.687	
RW1	L. glabella/L. cranidium	0.85	0.000	*
RW1	W. interocular genae/W. glabella (eyes)	−0.74	0.000	*
RW1	W. posterior fixigenae/W. occipital ring	−0.71	0.000	*
RW1	L. occipital ring/L. cranidium	0.36	0.003	
RW1	L. occipital ring/L. glabella	−0.23	0.066	
RW1	L. palpebral lobes/L. glabella	−0.59	0.000	*
RW1	Log (L. cranidium)	0.04	0.745	
RW2	L. preglabellar field/L. occipital ring	−0.16	0.208	
RW2	W. glabella (base)/L. glabella	0.39	0.002	*
RW2	L. glabella/L. cranidium	0.06	0.621	
RW2	W. interocular genae/W. glabella (eyes)	0.16	0.209	
RW2	W. posterior fixigenae/W. occipital ring	0.19	0.127	
RW2	L. occipital ring/L. cranidium	0.15	0.256	
RW2	L. occipital ring/L. glabella	0.11	0.392	
RW2	L. palpebral lobes/L. glabella	−0.08	0.523	
RW2	Log (L. cranidium)	0.12	0.341	

*Statistically significant.
L., length; W., width

P. clarisae presents a shorter preglabelar field, a poorly developed interocular genae and a long, forwardly narrower glabella, with a wide base. On the other hand, *P. pompadouris* shows an acuminate anterior margin, a divergent anterior branch of the facial suture, interocular genae moderately developed, and a posterior fixigenae narrow with a posterior branch of the facial suture more convex and directed posteriorly (Fig. 5.1). The *P. pompadouris* specimens from Bocoyá river present a less divergent anterior branch of the facial suture, a more developed preglabellar field and less developed interocular genae and the *P. pompadouris* specimens from Nazareno river and quebrada Moya show backwardly directed posterior fixigenae and slightly less developed interocular genae (Fig. 5.2).

Regarding the relation between the shape and the size when all the data is analysed together, the change in shape explained by the size is only 1.76% and the regression is not significant ($P = 0.33$). For each group, the regressions present no significative differences for *P. argentinensis* (3.57% explained variance; permutation test $P = 0.63$), *P. clarisae* (4.77% explained variance; permutation test $P = 0.14$) and *P. pompadouris* (16.99% explained variance; permutation test $P = 0.29$). So, there is not enough evidence to state that there is a variation in shape associated with size.

Discussion

Morphological variation is believed to be characterized by gaps between taxa. The presence of these gaps makes each taxon uniquely diagnosable (see Otte and Endler, 1989). However, this is not always so easy to assess, because there is a continuum of variation observed between different specimens. The intraspecific variation in fossil taxa without living representatives is in most cases difficult to identify. Classic and geometric morphometry provide a more rigorous assessment of the observed variation in a particular sample. In addition, those methods can distinguish between different sources of variation (e.g., Lawing and Polly, 2010). Thus, both classical and geometric morphometry proved to be a useful method to differentiate taxa (e.g., Hughes, 1994; Adrain and Westrop, 2006; Webster, 2009; Hopkins and Webster, 2009; Gendry et al., 2013; Pandey and Parcha, 2013). The use of geometric morphometry in systematic studies has increased in the past 10 years. Morphometrics can be used in taxonomic discrimination and can reveal new species. In the case of study of this work *Parabolinella argentinensis* s. s, *P. clarisae* n. sp. and *P. pompadouris* n. sp can be differentiated with both morphogeometric and classical morphometry, but the former analysis provides a graphical representation which in turn provides a clearer observation of the differences between the species. The three morphospecies can be separated with the function obtained by the Discriminant Analysis, but this mathematical descriptor is not always a character recognizable in the material, and cannot be used in the diagnoses. (Zelditch et al., 2004). In classic morphometry, the variables that separate the different species are easily recognizable on new specimens. In this case in particular, a clear separation between *P. clarisae* and the group of *P. argentinensis* + *P. pompadouris* is observed, but the distinction between *P. argentinensis* and *P. pompadouris* is less clear. So this method cannot be used to obtain diagnostic characters for this species. In the case of geometric morphometry, since the variables analyzed did not have a biological sense in itself, it is difficult to find characters to diagnose species. Nevertheless, because geometric morphometry provides a graphical representation, the Discriminant Analysis

https://doi.org/10.1017/jpa.2016.53 Published online by Cambridge University Press

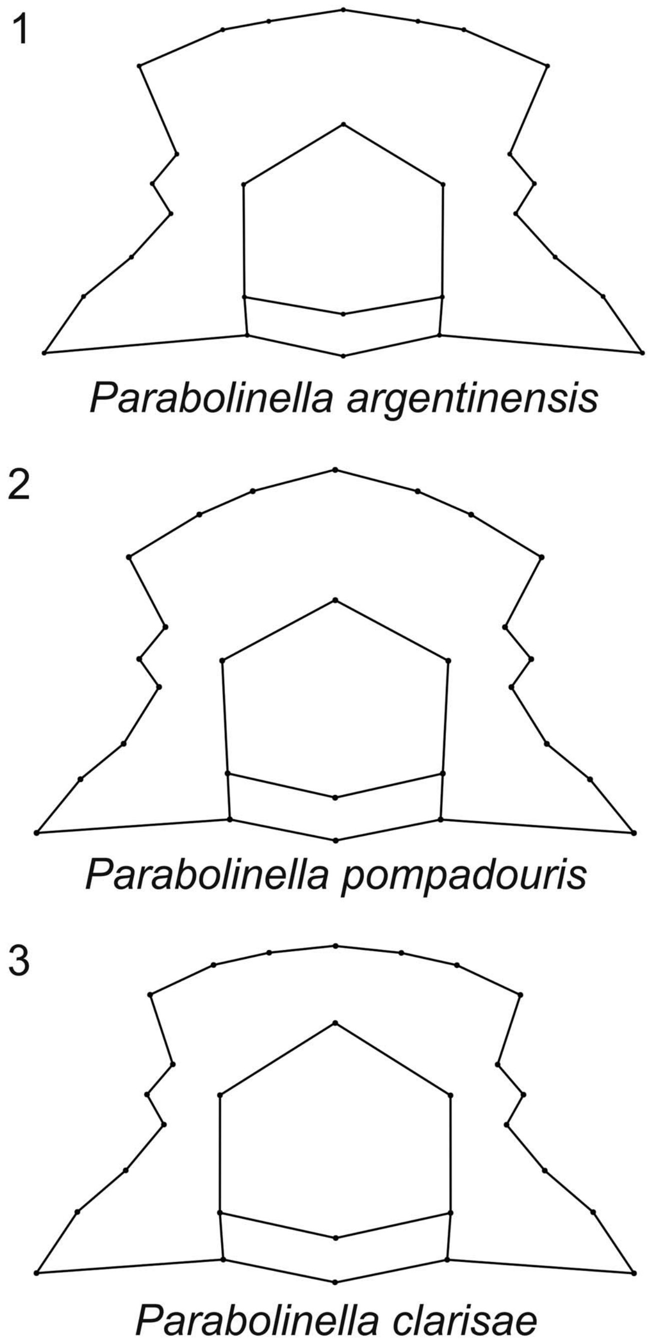

Figure 6. Consensus shape of each morphospecies. **(1)** *Parabolinella argentinensis* s.s. **(2)** *Parabolinella pompadouris* n. sp. **(3)** *Parabolinella clarisae* n. sp.

gives a consensus form for each morphospecies (Fig. 6). From these representations, qualitative characteristics that differentiate the three morphospecies, such as the shape of the anterior margin of the cranidium and the shape of the posterior branch of the facial suture, can be distinguished. Also from these consensus forms other characters expressed as classic morphometric variables, easier to recognize on the material, can be identified. In this sense, diagnostic characters that distinguish the three morphospecies can be determinate by the correlation between ratio variables and the principal components. A similar pattern is observed from the correlation between classical variables and RW1 and the PCA with classic variables. The quantifiable characteristics that distinguish *P. clarisae* from other species of *Parabolinella* are: length of the preglabellar field related to the length of occipital ring (95% confidence interval [CI] 1.64–1.91); width of the interocular genae related to the width of the glabella (eyes) (95% CI 0.3–0.33); width of the posterior fixigenae related to the width of the occipital ring (95% CI 0.74–0.79); length of the palpebral lobes related to the length of the glabella (95% CI 0.26–0.29); and the length of the glabella related to the length of the cranidium (95% CI 0.63–0.66). Geometric morphometry also allows a clearer separation of *P. pompadouris* from *P. argentinensis*, but there is no clear correlation with the classic variables considered. In this sense, it is noteworthy that qualitative characters are the most important to separate the two taxa. The differences between these two species, like the direction of the posterior branch of the facial suture and the form of the anterior margin, cannot be represented by classic morphometry variables, but can be clearly observed on the consensus form obtained by geometric morphometry.

As mentioned above, the species *Parabolinella argentinensis* s. Harrington and Leanza shows a great morphological variation (e.g., Waisfeld and Vaccari, 2003; Zeballo and Tortello, 2005). These results suggest that *Parabolinella argentinesis* s. Harrington and Leanza can be divided into three different morphospecies (*P. argentinensis* s. s., *P. clarisae*, and *P. pompadouris*). These three morphotypes were included, but not described, as different terminals in a previous phylogenetic analysis where they were recovered as different evolutionary lineages (Monti and Confalonieri, 2013; *P. pompadouris* = *P.* sp. 1; *P. clarisae* = *P.* sp. 2). Given that the results of the phylogeny alone are not enough to identify new species, the use of different methodological approaches and an exhaustive qualitative study helped to recognize morphological traits that can be used to distinguish and describe the three morphotypes. These results support the previous separation (Monti and Confalonieri, 2013) and show how the combination of different methods is useful in the resolution of taxonomic hypotheses, especially in fossil taxa, in which the morphological variation is the only source of information to identify different species.

The specimens of *P. pompadouris* where collected in three different localities of the same biozone (Harrington and Leanza, 1957; Tortello et al., 2013). The specimens from Bocoyá river show a less divergent anterior branch of the facial suture, a more developed preglabellar field and a less developed interocular genae, whereas those from Nazareno river and quebrada Moya has a more divergent anterior branch of the facial suture, wider intereocular genae and a less developed preglabellar field. These differences between specimens from different localities of the same age, suggest a correlation between the precedence of the material and the morphology of the specimens. This hypothesis needs to be tested in a further project that includes more specimens in the analyses.

The allometric growth is well documented in several species of olenids (e.g., Kim et al., 2002), but this allometry was found in specimens of different stages of development (ontogenetic allometry, Cook, 1966). This is not the case study here, where the specimens included are all holaspids. Thus, the type of allometric growth studied here is the static allometry which deals with covariation of traits within a particular ontogenetic stage of a single species (Cock, 1966; = individual allomorphosis Gould, 1966). This type of allometry was not explored particularly in other species of olenids. Exploratory analysis performed in other species of olenids from the Cordillera Oriental; e.g., *Jujuyaspis keideli* (Monti, 2013) and *Leptoplastides granulosus* (unpublished data, Monti, 2014) may indicate that this type of allometry can exist in holaspids of olenids. However, in the three species studied in this work, no relation between size and shape of the cranidium was observed. A correlation between the RW1 and an estimator of size (total length of the cranidium) was performed and its results (r(pearson) $= 0.07$; $P = 0.5973$) are congruent with the results of the regression, so it can be consider that there is no static allometry in the species studied here.

Repository and institutional abbreviation.—The studied specimens are deposited in the Invertebrate Paleontology Collection, Department of Geology (Paleontology area), Facultad de Ciencias Exactas y Naturales, Universidad de Buenos Aires.

Systematic paleontology

The proportions expressed in percentages in the descriptions and the diagnoses are median, with the range of values expressed between parentheses. All measurements were obtained from digital images using the Measure Tool of Adobe Photoshop.

Class Trilobita Walch, 1771
Order Ptychopariida Swinnerton, 1915
Suborder Olenina Burmeister, 1843
Family Olenidae Burmeister, 1843
Subfamily Oleninae Burmeister, 1843
Genus *Parabolinella* Brøgger, 1882

Type species.—*Parabolinella limitis* Brøgger, 1882 (Bassler, 1915) from upper Tremadocian of Scandinavia.

Parabolinella argentinensis Kobayashi, 1936
Figure 7.1–7.5

1936 *Parabolinella argentinensis* Kobayashi, p. 88, pl. 15, figs. 1–5
1937 *Parabolinella argentinensis*; Kobayashi, p. 406, pl. 4
1938 *Parabolinella argentinensis*; Harrington, p. 193–194, pl. 7, figs. 1, 2, 7, 8
1957 *Parabolinella argentinensis*; Harrington and Leanza (part), p. 104, 106, figs. 37.3, 37.10, 38.1, 38.3, 38.7
2003 *Parabolinella argentinensis*; Waisfeld and Vaccari, p. 330, pl. 32, figs. 9–13

Types.—Lectotype, elected by Henningsmoen, 1957, p.134: Cephalon with three thoracic segments figured by Kobayashi (1936, pl. 15, fig. 1) from the lower Tremadocian of the "Purmarca shales," east side of the Quebrada de Humahuaca, Jujuy.

Diagnosis.—*Parabolinella* that combines a striated, large preglabellar field (approximately 2.61–2.85 times larger than occipital ring) separated from the border by a deep, pitted marginal furrow; a wide interocular genae (approximately 0.45–0.47 of glabellar width) and a well-developed posterior fixigenae (almost equally width than occipital ring 0.97–1.04); anterior section of the facial suture divergent and a subquadrate short glabella, approximately 0.55–0.57 of the total cranidial length, with a narrow base and three glabellar furrows, S1 sigmoidal and bifurcated.

Occurrence.—Alfarcito Member, Santa Rosita Fomation, Purmamarca region and Rupasca Member, Santa Rosita Formation, quebrada San Gregorio (Tilcara). *Parabolinella argenitnensis* s.s. also ocurrs on La Caldera, Highway between Salta and Jujuy (S.Cal-3 (A3) of Harrington and Leanza, 1957) and Cerrillos, quebrada Pingüiyal (S.Cer-1 [PG 36] of Harrington and Leanza, 1957).

Description.—Dorsal exoskeleton elliptical in outline. Cephalon semicircular. Cranidium trapezoidal, twice as wide as long. Glabella subquadrate, almost as wide as long, well defined by subparallel deep axial furrows, anteriorly truncated, occupies 0.56 (0.55–0.57) of the total crainidial length (sag). Three pairs of glabellar furrows: S1 deep, forked and sigmoidal; S2 just convex, as long as S1; S3 divided into two sections, inner one faint slitlike, shallow, and transverse and outer one depressions elongated in the anterolateral corners of the glabella. S1 and S2 disconnected of the axial furrows. Preglabellar field well developed, 2.73 (2.61–2.85) times larger than occipital ring (sag.), striated, separated from the anterior border by a deep, pitted marginal furrow. Anterior border convex, occupying 0.23 (0.18–0.28) of the preglabellar field, medially enlarged (sag.). Ocular ridges prominent, transverse. Palpebral lobes moderately long, with a length (exasag.) equal to 0.38 (0.36–0.44) of the glabellar length (sag.). Centers of palpebral lobes aligned with S2. Interocular cheeks well developed, approximately 0.46 (0.45–0.47) of glabellar width at the eyes line (tr.). Anterior section of facial suture divergent (angle 40º). Posterior section of the facial suture sinuous, reaching the posterior margin far from the axial furrow, 0.98 (0.97-1.04) related to the width of the occipital ring. Posterior border narrower than occipital ring, 0.79 (0.66–0.84) its length (sag. to S0). Occipital ring small, approximately 0.22 (0.20–0.24) of the length of the glabella (sag.), compound by a crescentic medial portion and triangular lateral portions, with a prominent median tubercle. Librigenae convex and long with delicate anastomosing striae. Genal spine long, extending to the half of the thorax, continuing the curvature of lateral margin. Lateral border convex, defined by a deep lateral furrow.

Thorax with 21 segments; axis as wide as pleural fields (tr.), posteriorly narrower with each segment bearing a median node. Pleurae with proximal fulcrum, extremities ending in short spines, curved backward in the anterior region and becoming rounded towards the posterior part. Pleural spines striated. Pleural furrow straight.

Pygidium small (approximately 0.044 [0.042–0.046] of the total dorsal exoskeleton length [sag.]), semiellipical. Length (sag.) equal to 0.24; (0.20–0.30) of its width (tr.). Pigaxis short occupying 0.33 (0.31–0.37) of maximum width of the pygidium (tr.), narrowing backward, with one ring and a rounded terminal piece. Pleural fields with two strong and oblique pleural furrows and a faint interpleural groove. Margin entire, with medial posterior portion concave.

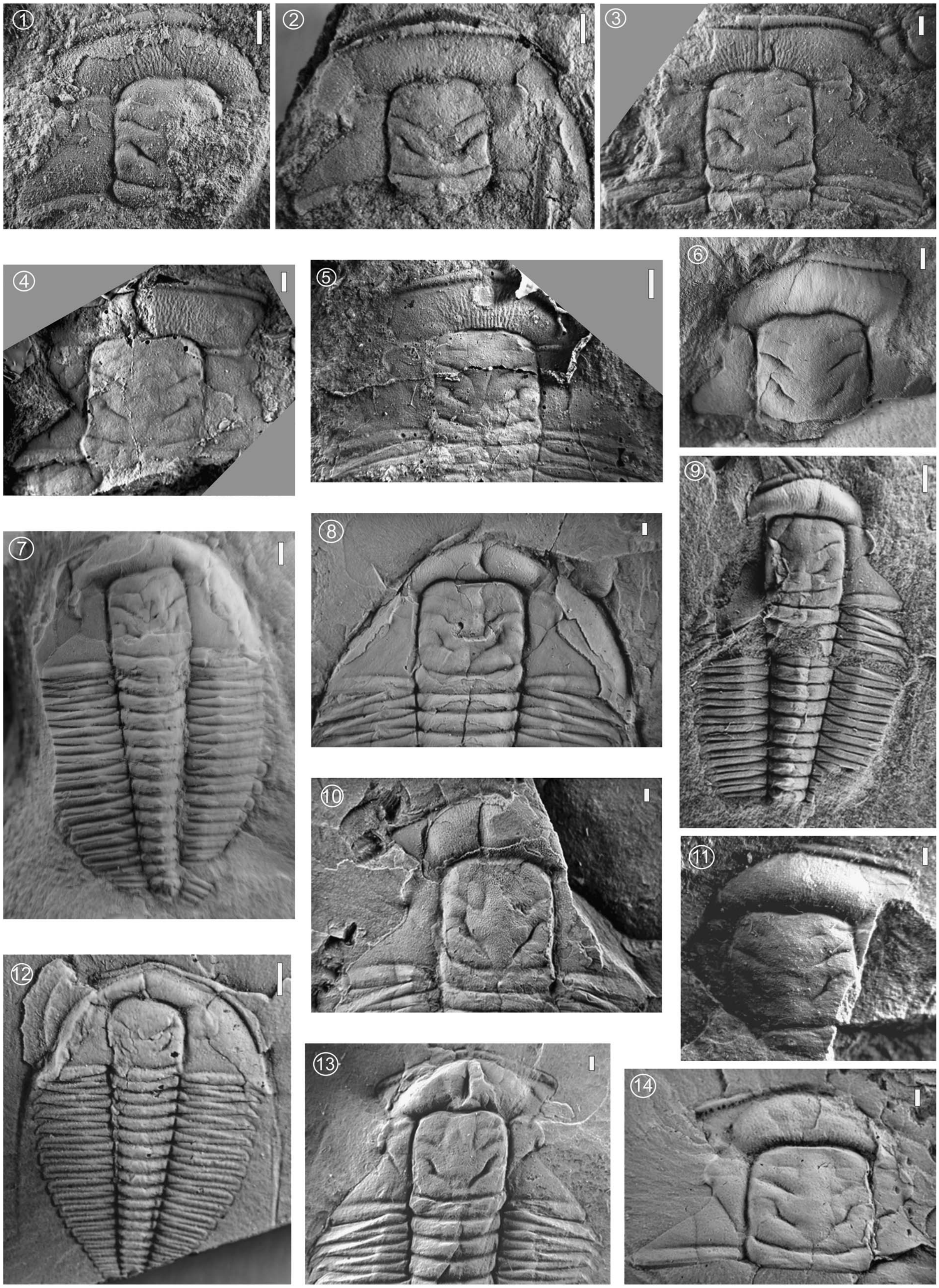

https://doi.org/10.1017/jpa.2016.53 Published online by Cambridge University Press

Remarks.—Harrington and Leanza (1957) included a great variety of morphologies in this species. In this paper its diagnosis is restricted to those specimens whose morphology corresponds to the original description of Kobayashi (1936) and the diagnosis is emended considering the results obtained from the morphometric analysis.

P. argentinensis is closely related to *P. triarthra* (Callaway, 1977) from the Furongian and Tremadocian of England South Wales, Eastern Canada and Tasmania; (Callaway, 1877, pl. XXVI, fig.6), *P. bolbifrons* Fortey and Owens, 1997 from the lower Tremadocian of Breadstone Shales (Fortey and Owens, 1997, pl. 1, figs. 1–8); and *P. limitis* Brøgger 1882 from the late Tremadocian of Scandinavia and Eastern Canada (Henningsmoen, 1957, pl.1, fig. 8; pl. 8; pl. 12, figs. 1–5). *Parabolinella argentinensis* differs from *P. triarthra* in having a striated, more developed preglabellar field, a divergent anterior section of the facial suture, and wider interocular genae. It is easily distinguishable from *P. bolbifrons* by having a shorter preglabellar field and lacking a frontal protuberance and from the type species *P. limitis* by showing a well-developed and striated preglabellar field, and wider interocular genae.

Parabolinella pompadouris new species
Figure 7.6–7.14

1957 *Parabolinella argentinensis* Kobayashi; Harrington and Leanza (part), p. 104, 106, 37, figs. 37.1, 37.2, 37.5, 37.6, 37.7, 38.4, 38.5, 38.6, 38.8

?1982 *Parabolinella argentinensis*; Owens et al., p. 8-9, pl. 1, figs. g, h, i

2005 *Parabolinella argentinensis*; Zeballo and Tortello, p. 135, pl. 4, figs. h–j, l, n

2013 *Parabolinella* sp.; Tortello et al., p. 145, figs.8.1, 8. 3–8.5, 8.8, 8.10

Holotype.—An almost complete specimen (CPBA 21644, Fig. 7.7) from the upper Alfarcito Member, Santa Rosita Formation, quebrada Moya.

Diagnosis.—*Parabolinella* with an inflated, very well-developed preglabellar field (approximately 3.48–3.82 times longer than occipital ring) anastomosing preglabellar striae, and a pitted anterior border furrow. Anterior margin acuminate.

Occurrence.—Plus the Type locality, *P. pompadouris* also occurs at Casa Colorada Member, Santa Rosita Formation, quebrada San Gregorio (Tilcara) and the lower part of Santa Rosita Formation at Nazareno river (Iruya) and Bocayá river (Santa Victoria), *Kainella meridionalis* Biozone.

Description.—Dorsal exoskeleton subelliptical, with its maximum width at the median region, posterior region almost triangular. Cephalon subelliptical, twice as wide as long. Cranidium subtrapezoidal, with an acuminate anterior margin. Gabella almost as wide as long, well defined by deep, subparallel or forwardly diverging axial furrows, anteriorly truncated, occupies approximately 0.54 (0.53–0.55) of the length of the cranidium (sag.). Three pairs of glabellar furrows, all disconnected from the axial furrows: S1 deep, forked, and sigmoidal; S2 almost as deep as S1 and equally long, straight and oblique; S3 shallower and slitlike. Anterolateral corners of the glabella with fossulae. Ocular ridges thin and transverse. The length of the palpebral lobes (exasag.) equal to 0.37 (0.34–0.38) of glabellar length (sag.). Preglabellar field inflated into a protuberance, more or less developed, with anastomosing radial striae, separated from the anterior border by a deep, pitted marginal furrow. Preglabellar field very well developed, 3.73 (3.48–3.82) times as long as the occipital ring (sag.). Anterior border narrow and convex, occupies 0.18 (0.11–0.24) of the preglabellar field (sag.), this relative length is higher in smaller specimens. Occipital ring compound by a crescentic medial portion and two triangular lateral portions, with a prominent median tubercle, length (sag.) equal to 0.18 (0.17–0.19) of the length of the glabella (sag.). Anterior section of facial suture divergent (angle 30º–40º) converging forwards before reaching the anterior cranidial margin. Posterior section of the facial suture convex and obliquely directed. Postocular fixigenae triangular, posteriorly almost as wide as occipital ring (approximately 0.88 [0.83–0.94] of the width of the occipital ring [tr.]). Posterior border slightly narrower than occipital ring (approximately 0.89 [0.77–0.98] of the occipital ring [sag.]). Interocular genae well-developed, relatively narrower in bigger specimens, approximately 0.38 (0.36–0.40) of the glabellar width at the eye line (tr.). Cranidium with tiny tubercles, except in the glabella. Librigenae very convex, twice as long as the maximum width. Lateral border slightly convex, defined by a deep lateral furrow that fades posterolateraly. Genal spine long, extending to three-fourths of the thorax, continuing the curvature of the lateral margin. Well-preserved specimens show the surface of the librigenae crossed by very delicate and irregular radial striae.

Thorax with at least 19 segments; axis narrowing backward, its width is approximately one third of the total width of the thorax; each segment bearing a prominent medial node. Pleurae with proximal fulcrum, extremities ending in short spines curved backward in the anterior region and becoming rounded towards the posterior part. Pleural spines striated. Pleural furrow straight or weakly concave anteriorly.

Pygidium unknown.

Figure 7. **(1–5)** *Parabolinella argentinensis* s. s. Kobayashi from the type locality, quebrada Salto Alto, Lower Tremadoc. All scale bars represent 1 mm. **(1)** Cranidium, note the medially enlarged anterior border (CPBA 21636–4). **(2)** Cranidium in dorsal view (CPBA 21637–1). **(3)** Cranidium in dorsal view (CPBA 4322). **(4)** Latex mold of the cranidium (CPBA 21637–2). **(5)** Latex mold of the cranidium (21635–2). **(6–14)** *Parabolinella pompadouris* n. sp. All scale bars represent 1 mm. **(6)** Cranidium with very convex preglabellar field and delicate stria (paratype), quebrada Moya (CPBA 21645–1). **(7)** Almost complete specimen (holotype), quebrada Moya (CPBA 21644). **(8)** Cranidium and anterior part of the thorax, Nazareno river (CPBA 3909). **(9)** Cranidiothorax, Nazareno river (CPBA 3917). **(10)** Crandium with a bubble head and granulate ornamentation, Nazareno river, (CPBA 3921). **(11)** Crandium with inflated preglabellar field (paratype), quebrada Moya (CPBA 21645–2). **(12)** An almost complete specimen Bocoyá river, (CPBA 4036). **(13)** Cranidium and anterior part of the thorax, Nazareno river (CPBA 3931). **(14)** Cranidium Bocoyá river, (CPBA 4036).

Etymology.—Named after the SS Madame de Pompadour, a fictional spaceship from the long-running science fiction program Doctor Who, given that the preglabellar field of this species resembles the pompadour hairstyle.

Remarks.—Some specimens assigned to this new species were previously regarded as *P. argentinensis* Kobayashi, 1936 by Harrington and Leanza (1957, figs. 37.1, 37.2, 37.5, 37.6, 37.7, 38.4, 38.5, 38.6). However, they differ from *P. argentinensis*, as revised herein, by having a large, inflated preglabellar field, with more delicate striae; an acuminate anterior border that is not expanded at the middle (sag.); narrower interocular genae; less divergent anterior sections of facial suture, and a tuberculate ornamentation on the cranidium; posterior fixigenae narrower and posterior branch of the facial suture more convex and directed posteriorly.

While *P. pompadouris* is characterized by a bulge in the preglabellar field, some variability is observed among the specimens described here. Some specimens show a very convex preglabellar field (Fig. 7.6, 7.12), other have a gently inflated preglabellar field (Fig. 7.7, 7.11, 7.14) and other show a bubble-like preglabellar field (Fig. 7.8–10, 7.13). However, they share unique features that distinguish them from other species of *Parabolinella*, which justify their inclusion in this new species. Also, the differences in the degree of development of the protuberance in the preglabellar field occurs at the same locality. Fortey and Hughes (1998) proposed the blunted preglabellar field as a sexual differentia describing it as broodpouches. The fact that specimens with different degrees of convexity in the preglabellar field occur at the same locality, is consistent with this idea.

Parabolinella pompadouris n. sp. differs from *P. bolbifrons* Fortey and Owens (1997, pl. 1, figs. 1–8) from the lower Tremadocian of Breadstone Shales in the nature of the protuberance of the preglabellar field, the first species present a preglabellar field separated from the border by a deep marginal furrow and the presence of anastomosing striae. The preglabellar field in *P. bolbifrons* is longer, approximately 4.5 times the length of the occipital ring. *Parabolinella* n. sp can be distinguished by an inflated preglabellar field. The specimens from North Wales described by Owens et al. (1982, pl. 1, figs. g, h, i), are characterized by a bulge in the preglabelar field and they possibly belong to this new species.

Parabolinella clarisae new species
Figure 8.1–8.11

1957 *Parabolinella argentinensis* Kobayashi; Harrington and Leanza (part), p. 104, figs. 37.4, 37.9, 37.11

?1968 *Parabolinella argentinensis*; Robinson and Pantoja-Alor, p. 789, pl. 102, fig. 5

?1980 *Parabolinella argentinensis*; Pribyl and Vanek, p. 18–19; pl. 7, figs. 1–2; pl. 8, fig. 8

Holotype.—An almost complete specimen (CPBA 4167, Fig. 8.2) from Alfarcito Member, Santa Rosita Formation, quebrada Rupasca (Tilcara), illustrated by Harrington and Leanza (1957, fig. 37.11).

Diagnosis.—*Parabolinella* with a well-developed preglabellar field (length approximately 1.64–1.91 of the length of occipital ring) crossed by delicate striae, narrow interocular genae (approximately 0.30-0.33 of glabellar width); posterior fixigenae approximately equal to 0.74–0.79 the width of the occipital ring; tiny palpebral lobes (approximately 0.26–0.29 of total glabellar length) and a large glabella (approximately 0.63–0.66 of total cranidial length).

Occurrence.—Plus the type locality, *Parabolinella clarisae* is recorded at Alfarcito Member, Santa Rosita Formation in Purmamarca region and quebrada San Gregorio (Tilcara). *P. clarisae* also occurs in lower Tremadocian of Reyes river (J.Cap-1 of Harrington and Leanza, 1957), Negrito river (S.Ora-5 of Harrington and Leanza, 1957) and Santa Victoria river (S.Vic-19 of Harrington and Leanza, 1957).

Description.—Dorsal exoskeleton elliptical. Cephalon semi-elliptical. Cranidium trapezoidal, twice as wide as long. Glabella turberculate (only seen on well-preserved specimens), subquadrate, almost as wide as long, well defined by subparallel or converging forward deep axial furrows, anteriorly truncated, it occupies 0.66 (0.63–0.66) of the total cranidial length (sag.). Three pairs of glabellar furrows: S1 deep, curved and forked; S2 less impressed, straight and oblique, almost as long as S1; S3 divided into two disconnected sections, external depressions elongate in the anterolateral corners of the glabella, internal sections faintly slitlike, shallow and transverse. S1 and S2 disconnected from the axial furrows. Preglabellar field striated, very convex in some specimens, separated from the anterior border by a deep marginal furrow with tiny pits. Preglabellar field approximately 1.71 (1.64–1.91) as long (sag.) as occipital ring (sag.), its relative length is minor in small specimens. Anterior border convex, occupying 0.15 (0.20 to 0.28) of the preglabellar field (sag.). Ocular ridges prominent, wide and oblique. Palpebral lobes small, with a length (exsag.) equal to 0.27 (0.26–0.29) of the glabellar length (sag.), reaching from L2 to opposite S3. Centers of palpebral lobes opposite to S2. Interocular cheeks moderately developed, approximately 0.32 (0.3–0.33) of the width of the glabella at the eyes line (tr.). Anterior section of facial suture slightly divergent (angle of 20º–30º). Posterior section of the facial suture slightly sinuous, cutting the posterior margin relatively far from the axial furrow (0.76 [0.74–0.79] related to the width of the occipital ring). Posterior border narrower than occipital ring, 0.71 (0.67–0.87) its length (sag. to S0). Occipital ring long, approximately 0.2 (0.20–0.21) of the length of the glabella (sag.), compound by a crescentic medial portion and two triangular lateral portions, with a prominent median tubercle. Librigenae convex and long with delicate anastomosing striae. Genal spine long, extending to ½ of the thorax, continuing the curvature of the cephalic lateral margin. Lateral border convex, defined by a deep lateral furrow, posterolaterally faint.

Thorax incomplete, with at least 19 segments; axis as wide as pleural fields, posteriorly narrower with each segment bearing a tubercle. Pleural extremities ending in short spines that are curved backward in the anterior region and become rounded towards the posterior part. Pleural spines striated. Pleural furrows slightly curved backward.

Pygidium unknown

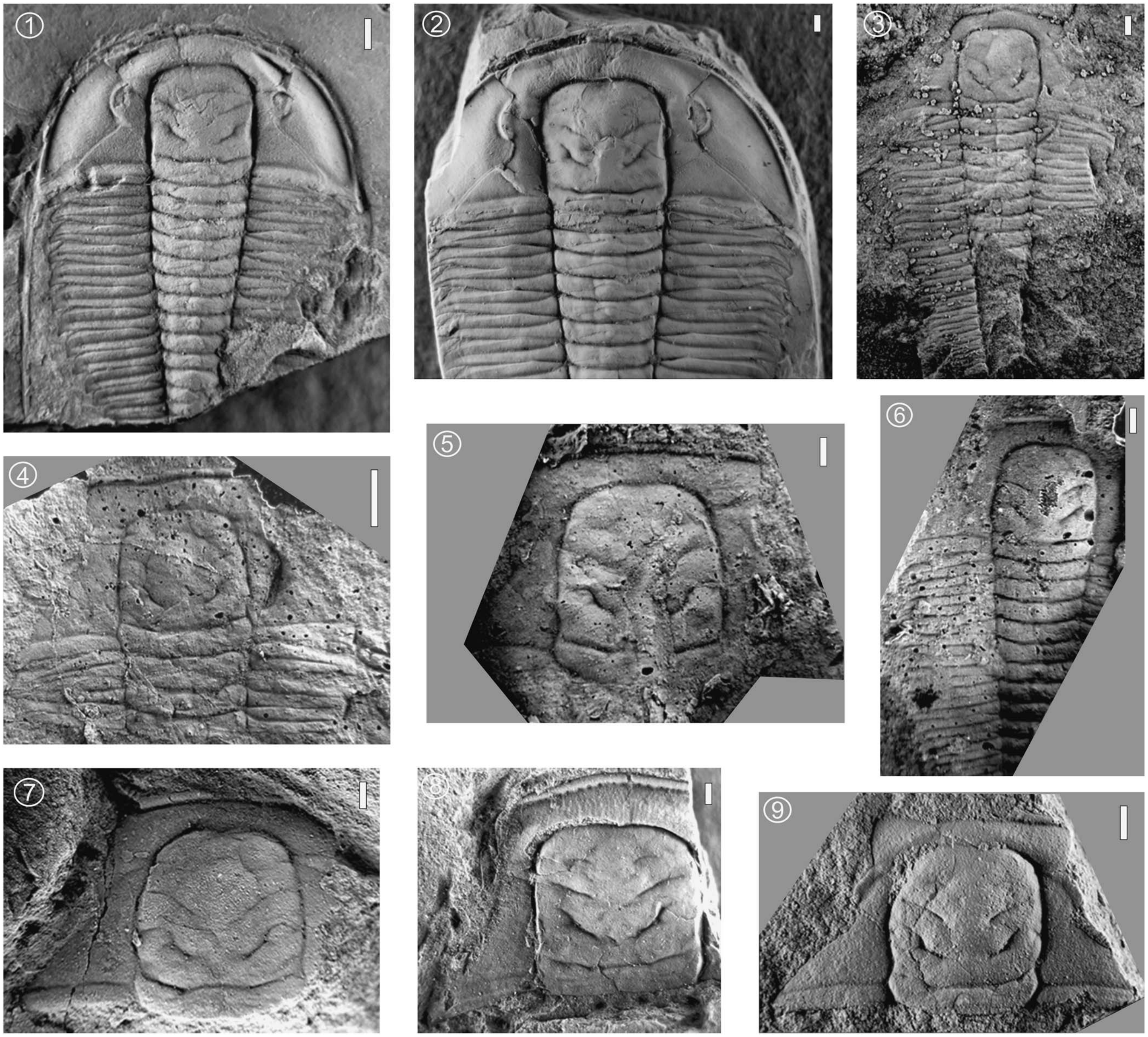

Figure 8. *Parabolinella clarisae* n. sp. **(1)** Almost complete specimen (paratype), quebrada Rupasca (CPBA 4166). **(2)** Cephalothorax (Holotype), quebrada Rupasca (CPBA 4167). **(3)** Cranidiothorax, quebrada Salto Alto (CPBA 1015). **(4)** Cranidium and anterior part of the thorax (latex mold) (CPBA 21630–5). **(5)** Latex mold of the cranidium (CPBA 21634–1). **(6)** Latex mold of a cranidiothorax (CPBA 21630-9). **(7)** Cranidium, quebrada Salto Alto (CPBA 21634–2). **(8)** Cranidium, quebrada Rupasca (CPBA 4190). **(9)** Cranidium, quebrada Salto Alto (CPBA 21638–2). All scale bars represent 1 mm.

Etymology.—Named after Clarisa, the daughter of D.S. Monti.

Remarks.—Though some specimens of *Parabolinella clarisae* were originally described as *P. argentinensis* Kobayashi, 1936 by Harrington and Leanza (1957, p. 104, figs. 37.4, 37.9, 37.11) they differ from the latter species, as revised herein (see above), by having a shorter preglabellar field, less developed interocular genae, less divergent anterior sections of the facial suture, and narrower posterior fixigenae.

Parabolinella clarisae n. sp. differs from *P. triarthra* (Callaway, 1877) from the upper Furongian and Tremadocian of England, South Wales, Eastern Canada and Tasmania (Callaway, 1877, pl. XXVI, fig. 6) by having an anteriorly narrower glabella, a shorter preglabellar field, well developed preglabellar striae, and divergent anterior sections of the facial suture. It can be distinguished from *P. limitis* Brøgger, 1882 from the late Tremadocian of Scandinavia and Eastern Canada (Henningsmoen, 1957, pl.1, fig. 8; pl. 8; pl. 12, figs. 1–5) by the presence of an anteriorly narrower and truncated glabella, a striated preglabellar field and a relatively wider occipital ring. *P. clarisae* n. sp differs from *P. tumifrons* Robison and Pantoja-Alor, 1968 from the Furongian - early Tremadocian of Mexico (Robison and Pantoja-Alor 1968, pl. 102, figs. 10-16), *P. prolata* Robison and Pantoja-Alor 1968 from the Furongian – early Tremadocian of Canada and Mexico (Robison and Pantoja-Alor 1968, pl. 102, figs. 3, 6, 9) and *P. lata* Henningsmoen (1957, pl. 8, pl. 12, fig. 8) from the late Tremadocian of Scandinavia in having three pair of glabellar furrows instead of two. It also differs from *P. variabilis*

https://doi.org/10.1017/jpa.2016.53 Published online by Cambridge University Press

Robison and Pantoja-Alor from the Furongian - early Tremadocian of Mexico (Robison and Pantoja-Alor 1968, pl. 102, figs. 17–21) by the presence of divergent anterior sections of the facial suture, a punctuated anterior border furrow, a well-defined glabellar furrows and wider interocular genae. *P. clarisae* n. sp. distinguishes from *P. ocellata* Lu and Lin (1984, pl. IX, figs. 6–8), *P. hunanensis* Peng (1991, pl. II, figs. 4–5) and *P. jiagnanensis* Lu and Lin (1984, pl. VII, figs. 10–13; pl. IX, figs. 1–5), from the early Tremadocian of China, by showing a pitted anterior marginal furrow an anteriorly truncated glabella, a stronger glabellar furrows, narrower interocular genae and oblique eye ridges. It differs from *P. bolbifrons* Fortey and Owens (1997, pl. 1, figs. 1–8) from the lower Tremadocian of Breadstone Shales by a shorter, not inflated preglabellar field. It can be distinguished from *P. coelatifrons* Harrington and Leanza (1957, figs. 39.3a–h) from the late Furongian of Argentine by having an anterior facial suture that is divergent instead of subparallel, a sinuous posterior facial suture, narrower posterior fixigenae.

Conclusions

Both classic and geometric morphometry analyses showed similar results, but the latter distinguishes more clearly the three morphotypes. While classic morphometry have the advantage that the variables used for the analysis are easily determinable on new material, the latter provide a graphical representation of the differences between the observed groups. From those representations plus the correlation between classical variables and principal components, diagnostic characters that distinguish the three morphospecies emerge. Three groups can be distinguished within *Parabolinella argentinensis* s. Harrington and Leanza: *Parabolinella argentinensis* s. s. is characterized by a well-developed preglabellar field (length related to the occipital ring, 95% CI 2.61–2.85), wide interocular genae (width related to the glabella, 95% CI 0.45–0.47), and a short (length related to the cranidium, 95% CI 0.55–0.57), subsquared glabella with a narrow base; *Parabolinella clarisae* n. sp. shows a poor development of the preglabellar field (length related to the occipital ring, 95% CI 1.64–1.91) and the interocular genae (width related to the glabella 0.3-0.33, at 95% of confidence), and a long glabella with a wide base (length related to the cranidium, 95% CI 0.74–0.79); *Parabolinella pompadouris* n. sp. combines a well-developed preglabellar field (length related to the occipital ring, 95% CI 3.48–3.82) with an acuminate anterior margin, a divergent anterior branch of the facial suture, with an interocular genae moderately developed (width related to the glabella, 95% CI 0.36-0.40), and a narrow posterior fixigenae (width related to the glabella, 95% CI 0.83–0.94) with a posterior branch of the facial suture more convex and directed posteriorly. The specimens of *P. pompadouris* n. sp show some degree of intraspecific variation correlated with the localities where they were found. Finally, there is no allometric growth for any of these three species.

Acknowledgments

We thank F. Tortello and V. Confalonieri for carefully reading an early version of the manuscript and for giving valuable comments and advices. Thanks are also due to B. Aguirre-Urreta and M. Tanuz of the Facultad de Ciencias Exactas y Naturales, Universidad de Buenos Aires (Argentina) for the loan of material in their care. We thank J. Carlucci, two anonymous reviewers and the Editors, S. Westrop and B. Pratt for improving the quality of the work. Finally we acknowledge to CONICET and Universidad de Buenos Aires for financial support.

References

Abe, F.R., and Lieberman, B.S., 2012, Quantifying morphological change during an evolutionary radiation of Devonian trilobites: Paleobiology, v. 38, p. 292–307.

Aceñolaza, G.F., 1996, Presencia de *Rhabdinopora* (Graptolothina) en la Quebrada de Humahuaca, provincial de Jujuy: Ameghiniana, v. 33, p. 95–98.

Aceñolaza, F.G., and Aceñolaza, G.F., 1992, The genus *Jujuyaspis* as a world reference fossil for the Cambrian–Ordovician boundary, *in* Webby, B., and Laurie, J.R. eds., Global Perspectives on Ordovician Geology: Rotterdam, Balkema, p. 115–120.

Aceñolaza, G.F., and Albanesi, G.L., 1997, Conodont–trilobite biostratigraphy of the Santa Rosita Formation (Tremadoc) from Chucalezna, Cordillera Oriental, northern Argentina: Ameghiniana, v. 34, p. 113.

Aceñolaza, G.F., Tortello, M.F., and Rábano, I., 2001, The eyes of the early Tremadoc Olenid trilobite *Jujuyaspis keideli* Kobayashi, 1936: Journal of Paleontology, v. 75, p. 346–350.

Adrain, J.M., and Westrop, S.R., 2006, New earliest Ordovician trilobite genus *Millardicurus*: the oldest known hystricurid: Journal of Paleontology, v. 80, p. 650–671.

Aráoz, L., and Vargel, M.M., 2006, Palinología de la transición Cambro–Ordovícica en quebrada de Moya, Cordillera Oriental, Argentina: Revista Brasileira de Paleontología, v. 9, p. 1–8.

Bassler, R.S., 1915, Bibliographic index of American Ordovician and Silurian fossils: Bulletin of the United States National Museum, v. 92, p. 1–152.

Bao, J-S., and Jago, J.B., 2000, Late Cambrian trilobites from near Birch Inlet, South–Western Tasmania: Palaeontology, v. 43, p. 881–917.

Bookstein, F.L., 1991, Morphometric Tools for Landmark Data: Geometry and Biology, Cambridge University Press, 435 p.

Bookstein, F.L., 1996, Applying landmark methods to biological outline data, *in* Mardia, K.V., Gill, C.A., and Dryden, I.L. eds., Image Fusion and Shape Variability: Leeds, UK, University Press, p. 59–70.

Bookstein, F.L., 1997, Landmark methods for forms without landmarks: morphometrics of group differences in outline shape: Medical Image Analysis, v. 1, p. 97–118.

Bookstein, F.L., Streissguth, A.P., Sampson, P.D., Connor, P.D., and Barr, H.M., 2002, Corpus callosum shape and neuropsychological deficits in adult males with heavy fetal alcohol exposure: Neuroimage, v. 15, p. 233–251.

Brøgger, W.C., 1882, Die Silurischen Etagen 2 und 3 im Kristianiagebiet und auf Eker: Universitats Programm 32, semestre 1882, Kristiania, p. 1–376.

Buatois, L.A., and Mángano, M.G., 2003, Sedimentary facies, depositional evolution of the Upper Cambrian–Lower Ordovician Santa Rosita Formation in Northwest Argentina: Journal of South America Earth Sciences, v. 16, p. 343–363.

Buatois, L.A., Zeballo, F.J., Albanesi, G.L., Ortega, G., Vaccari, N.E., and Mángano, M.G., 2006, Depositional environments and stratigraphy of the Cambrian–Tremadocian Santa Rosita Formation at the Alfarcito area, Cordillera Oriental, Argentina: Integration of biostratigraphic data within a sequence stratigraphic framework: Latin American Journal of Sedimentology and Basin Analysis, v. 13, p. 65–94.

Burmeister, H., 1843, Dier organisation der Trilobiten, aus ihrem lebenden Verwandten entewickelt; nebst einer systematischen übersicht aller zeither beschriebenen Arten: Berlin, 147 p.

Callaway, C., 1877, On a new area of Upper Cambrian rocks in south Shropshire, with a description of a new fauna: Quaternary Journal of the Geological Society of London, v. 33, p. 652–672.

Crônier, C., Auffray, J.-C., and Courville, P., 2005, A quantitative comparison of the ontogeny of two closely–related Upper Devonian phacopid trilobites: Lethaia, v. 38, p. 123–135.

Cock, A.G., 1966, Genetical aspects of metrical growth and form in animals: Quarterly Review of Biology, p. 131–190.

Di Cunzolo, S., Aceñolaza, G.F., and Rodríguez Brizuela, R., 2003, *Cruziana–Skolithos* ichnoassociation in the Casa Colorada Formation (Upper Cambrian–Tremadocian), Cordillera Oriental of Jujuy province, NW Argentina, *in* Albanesi, G.L., Beresi, M.S., and Peralta, S.H. eds., Ordovician from the Andes, INSUGEO: Serie Correlación Geológica, v. 17, p. 285–288.

Di Cunzolo, S.C., and Alfaro, M., 2008, Primer registro de *Rhabdinopora* cf. *praeparabola* Erdtmann (Graptolithina, Tremadociano inferior) para Sudamérica: 17º Congreso Geológico Argentino, Jujuy, Abstracts, p. 345–346.

Di Rienzo, J.A., Casanoves, F., Balzarini, M.G., Gonzalez, L., Tablada, M., and Robledo, C.W., InfoStat versión 2014: Grupo InfoStat, FCA, Córdoba, Argentina, Universidad Nacional de Córdoba.

Dryden, I.L., and Mardia, K.V., 1998, Statistical Shape Analysis: Chichester, England, John Wiley and Sons, 347 p.

Fortey, R.A., and Hughes, N.C., 1998, Brood pouches in trilobites: Journal of Paleontology, v. 72, p. 638–649.

Fortey, R.A., and Owens, R.M., 1997, Bubble–headed Trilobites, and a new olenid example: Palaeontology, v. 40, p. 451–459.

Green, J., 1832, A monograph of the trilobites of North America: with coloured models of the species: Philadelphia, J. Brano, 93 p.

Green, W.D.K., 1996, The thin-plate spline and images with curving features, *in* Mardia, K.V., Gill, C.A., and Dryden, I.L. eds., Image Fusion and Shape Variability: Leeds, United Kingdom, University Press, p. 79–87.

Gendry, D., Courville, P., Saucède, T., Laffont, R., and Paris, F., 2013, Contribution of Morphometrics to the Systematics of the Ordovician Genus *Neseuretus* (Calymenidae, Trilobita) from the Armorican Massif, France: Journal of Paleontology, v. 87, p. 456–471.

Goodall, C., 1991, Procrustes methods in the statistical analysis of shape: Journal of the Royal Statistical Society, Series B, v. 53, p. 285–339.

Gould, S.J., 1966, Allometry and size in ontogeny and phylogeny: Biological Reviews, v. 41, p. 587–638.

Gunz, P., Mitteroecker, P., and Bookstein, F.L., 2005, Semilandmarks in three dimensions, *in* Slice, D.E. ed., Modern Morphometrics in Physical Anthropology: New York, Springer, p. 73–98.

Hammer, Ø., Haper, D.A.T., and Ryan, P.D., 2001, PAST: Paleontological Statistics sofware package for education and data analysis: Paleontología Electrónica, v. 4, no. 1, p. 1–9.

Harrington, H.J., 1937, On some fossils from northern Argentina: Geological Magazine, v. 74, p. 97–124.

Harrington, H.J., 1938, Sobre las faunas del Ordovícico Inferior del norte argentino: Revista Museo de La Plata (n.s) Sección Paleontología, v. 4, p. 209–289.

Harrington, H.J., and Leanza, A.F., 1943, La fáunula del Tremadociano inferior de Salitre, Bolivia: Revista del Museo de La Plata, nueva serie (sección Paleontología), v. 2, p. 343–356.

Harrington, H.J., and Leanza, A.F., 1952, La clasificación de los "Olenidae" y de los Ceratopygidae" (Trilobita): Revista de la Asociación Geológica Argentina, v. 7, p. 190–205, 1 pl.

Harrington, H.J., and Leanza, A.F., 1957, Ordovician trilobites of Argentina: Lawrence, Kansas, University of Kansas: Special Publication, v. 1, 276 p.

Henningsmoen, G., 1957, The trilobite family Olenidae, with description of Norwegian material and remarks on the Olenid and Tremadocian Series: Skrifter Utgitt av det Norske Videnskaps-Akademi i Oslo I Matematisk-Naturvidenskapelig Klasse 1957, v. 1, 30 p.

Hopkins, M.J., and Webster, M., 2009, Ontogeny and geographic variation of a new species of the corynexochine trilobite Zacanthopsis (Dyeran, Cambrian): Journal of Paleontology, v. 83, p. 524–547.

Hughes, N.C., 1994, Ontogeny, intraspecific variation, and systematics of the Late Cambrian trilobite *Dikelocephalus*: Smithsonian Contributions to Paleobiology, v. 79, p. 1–89.

Hughes, N.C., and Chapman, R.E, 2001, Morphometry and Phylogeny in the Resolution of Paleobiological Problems — Unlocking the evolutionary significance of an assemblage of Silurian Trilobites, *in* Adrain, J.M., Edgecombe, G.D., and Lieberman, B.S. eds., Fossils, Phylogeny, and Form, v. 19 of Topics in Geobiology: New York, Kluwer Academic/Plenum Publishers, p. 29–54.

Kayser, E., 1876, Uber primordiale und untersilurische Fossilien aus der Argentinischen Republik. Palaeontographica, Supplementun 3, Lieferung 2, Theil III: Actas de la Academia Nacional de Ciencias, v. 8, p. 297–332.

Kayser, E., 1897, Beitrage zur Kenntniss einiger palazoischer Faunnen Sud-Amerikas: Zeitschr. d. Deutsch: Ceol. Gessels., Bd., v. 49, p. 274–317.

Keidel, J., 1925, Sobre el desarrollo paleogeográfico de las grandes unidades geológicas de la Argentina: Sociedad Argentina de Estudios Geográficos, GAEA, Anales, v. 4, p. 251–312.

Kim, K., Sheets, H.D., Haney, R.A., and Mitchel, C.E., 2002, Morphometric analysis of ontogeny and allometry of the Middle Ordovician trilobite *Triarthrus becki*: Paleobiology, v. 28, p. 364–377.

Kim, K., Sheets, H.D., and Mitchell, C.E., 2009, Geographic and stratigraphic change in the morphology of *Triarthrus beckii* (Green) (Trilobita): A test of the Plus ça change model of evolution: Lethaia, v. 42, p. 108–125.

Kobayashi, T., 1936, On the *Parabolinella* fauna from Jujuy Province, Argentina: Japanese Journal of Geology and Geography, v. 13, p. 85–102.

Kobayashi, T., 1937, The Cambro-Ordovician Shelly Faunas of South America: Journal of the Faculty of Science, Imperial University of Tokio, Section II, v. 4, p. 369–522.

López, C.R., and Nullo, F.E., 1969, Geología de la margen izquierda de la Quebrada de Humahuaca, de Huacalera a Maimará. Departamento Tilcara- Provincia de Jujuy, República Argentina: Revista de la Asociación Geológica Argentina, v. 24, p. 173–182.

Lu, Y-H., and Lin, H-L., 1984, Late late Cambrian and earliest Ordovician trilobites of Jianghan–Changsshan Area, Zhejiang, *in* Stratigraphy and Palaeontology of systemic boundaries in China, Cambrian-Ordovician boundary: Nanjing, China, Anhui Science and Technology Publishing House, v. 1, p. 45–143.

Ludvigsen, R., 1982, The Cambrian–Ordovician boundary in the western Distric of Mackensie, Canada, *in* Bassett, M. G., and Dean, W.T. eds., The Cambrian-Ordovician Boundary: Sections, Fossil Distributions, and Correlations, National Museum of Wales, Geological Series Nº3, Cardiff, p. 141–153.

Mángano, M.G., Buatois, L.A., and Aceñolaza, G.F., 1996, Trace fossils and sedimentary facies from an Early Ordovician tide–dominated shelf (Santa Rosita Formation, northwest Argentina): implications for ichnofacies models of shallow marine successions: Ichnos, v. 5, p. 53–88.

Mutanen, M., and Pretorius, E., 2007, Subjective visual evaluation vs. traditional and geometric morphometrics in species delimitation: a comparison of moth genitalia: Systematic Entomology, v. 32, p. 371–386.

Monti, D.S., 2013, Análisis morfogeométrico de *Jujuyaspis Keideli* Kobayashi (Trilobita, Olenidae) del Ordovícico Temprano del Noroeste Argentino: Ameghiniana, v. 50 (6r): suplemento resúmenes, p. R31.

Monti, D.S., and Confalonieri, V.A., 2013, Phylogenetic analysis of the late Cambrian-early Ordovician genus *Parabolinella* Brøgger (Trilobita, Olenidae): Geological Journal, v. 48, p. 156–169.

Moya, M.C., 1988, Lower Ordovician in the southern part of the Argentine Eastern Cordillera: Lecture Notes in Earth Sciences, v. 17, p. 55–69.

Otte, D., and Endler, J.A., 1989, Speciation and its consequences: Sunderland, Massachusetts: Sinauer Associates.

Owens, R.M., Fortey, R.A., Cope, J.C.W., Rushton, A.W.A., and Bassett, M.G., 1982, Tremadoc faunas from the Carmarthen district, South Wales: Geological Magazine, v. 119, p. 1–38.

Pandey, S., and Parcha, S.K., 2013, Systematics, Biometry of the species Opsidiscus from the Middle Cambrian succession of the Spiti Basin, India: Journal of the Geological Society of India, v. 82, p. 330–338.

Peng, S., 1991, Tremadocian trilobites from Goutang Formation, Luxi, Western Hunan: Acta Palaeontologica Sínica, v. 30, p. 141–166.

Pérez, S.I., Bernal, V., and González, P., 2006, Differences between sliding semi-landmark methods in geometric morphometrics, with an application to human craniofacial and dental variation: Journal of Anatomy, v. 208, p. 769–784.

Pribyl, A., and Vanek, J., 1980, Ordovician trilobites of Bolivia: Rozpravy Ceskoslovenské Akademie Ved, v. 90, p. 1–90.

Robison, R.A., and Pantoja-Alor, J., 1968, Tremadocian trilobites from the Nochixtlán region, Oaxaca, Mexico: Journal of Paleontology, v. 42, p. 767–800.

Rohlf, F.J., 1999, Shape statistics: procrustes method for the optimal superimposition of landmarks: Systematic Zoology, v. 39, p. 40–59.

Rohlf, F.J., 2010a, Tpsdig version 2.16, Department of Ecology and Evolution, State University of New York. http://life.bio.sunysb.edu.morph/. (accessed 23 June 2016).

Rohlf, F.J., 2010b, Tpsrelw version 1.49, Department of Ecology and Evolution, State University of New York. http://life.bio.sunysb.edu.morph/. (accessed 23 June 2016).

Rohlf, F.J., 2011, TpsRegr, ver. 1.41, Department of Ecology and Evolution, State University of New York. http://life.bio.sunysb.edu.morph/. (accessed 23 June 2016).

Rubinstein, C., Mángano, M.G., and Buatois, L.A., 2003, Late Cambrian acritarchs from the Santa Rosita Formation: implications for the recognition of the Cambrian-Ordovician boundary in the Eastern Cordillera of northwest Argentina: Revista Brasileira de Paleontología, v. 4, p. 43–48.

Shaw, A.B., 1951, The palaeontology of Northwestern Vermont 1: New Later Cambrian trilobites: Journal of Paleontology, v. 25, p. 97–114.

Sheets, H.D., 2014, TwoGroup8, Department of Physics, Canisius College, Buffalo, New York: http://www3.canisius.edu/~sheets/IMP%208.htm. (accessed 23 June 2016).

Swinnerton, H.H., 1915, II. Suggestions for a Revised Classification of Trilobites: Geological Magazine (Decade VI), v. 2, p. 538–545.

Terfelt, F., and Ahlgren, J, 2009, The first remopleuridioidean trilobite and the earliest *Parabolinella* species recorded in the Furongian of Scandinavia: Journal of Paleontology, v. 83, p. 299–306.

Tortello, M.F., and Aceñolaza, G.F., 1999, Trilobites agnóstidos del Ordovícico basal en la localidad de Purmamarca, Provincia de Jujuy, Argentina: Temas Geológico-Mineros ITGE, v. 26, p. 585–588.

Terfelt, F., and Ahlgren, J., 2009, The first remopleuridioidean trilobite and the earliest Parabolinella species recorded in the Furongian of Scandinavia: Journal of Paleontology, v. 83, p. 299–306.

Tortello, M.F., Zeballo, F.J., and Esteban, S. B., 2013, Trilobites tremadocianos en facies de lutitas oscuras del Miembro Alfacito (Formación Santa Rosita), Quebrada de Moya, Jujuy, Argentina: Ameghiniana, v. 50, p. 137–152.

Turner, J., 1960, Estratigrafía de la Sierra de Santa Victoria y adyacencias: Boletín de la Academia Nacional de Ciencias de Córdoba, v. 41, p. 163–196.

Vergel, M.M., Aceñolaza, G.F., and Aráoz, L., 2007, La Formación Casa Colorada en la quebrada de Moya (Cambro–Ordovícico): aportes a la cronoestratigrafía de una localidad clásica de la Cordillera Oriental de Jujuy (Argentina): Ameghiniana, v. 44, p. 621–630.

Waisfeld, B.G., and Vaccari, N.E., 2003, Trilobites, *in* Benedetto, J.L. ed., Ordovician Fossils of Argentina: Córdoba, Argentina, Secretaría de Ciencia y Tecnología, Universidad Nacional de Córdoba, p. 295–409.

Walch, J.E.I., 1771, Die Naturgeschichte der Versteinerungen, Dritter Theil: Paul Jonathan Felstecker, p. 1–235.

Webster, M., 2007, Ontogeny and evolution of the Early Cambrian trilobite genus *Nephrolenellus* (Olenelloidea): Journal of Paleontology, v. 81, p. 1168–1193.

Webster, M., 2009, Systematic revision of the Cambrian trilobite *Bathynotus* Hall, 1860, with documentation of new occurrences in western Laurentia and implications for intercontinental biostratigraphic correlation: Memoirs of the Association of Australasian Palaeontologists, v. 37, p. 369–406.

Webster, M., 2011, The structure of cranidial shape variation in three early ptychoparioid trilobite species from the Dyeran-Delamaran (traditional “lower-middle” Cambrian) boundary interval of Nevada, U.S.A.: Journal of Paleontology, v. 85, p. 179–225.

Webster, M., and Sheets, H.D., 2010, A practical introduction to landmark-based geometric morphometrics, *in* Alroy, J. and Hunt, G. eds., Quantitative Methods in Paleobiology: The Paleontological Society Papers, v. 16, p. 163–188.

Westergård, H.A., 1922, Sveriges Olenidskiffer. Sveriges geologiska undersokning: Serie Ca., v. 18, p. 1–205.

Zeballo, F.J., and Albanesi, G.L., 2013, New conodont species and biostratigraphy of the Santa Rosita Formation (upper Furongian-Tremadocian) in the Tilcara Range, Cordillera Oriental of Jujuy, Argentina: Geological Journal, v. 48, p. 170–193.

Zeballo, F.J., and Albanesi, G.L., 2009, Conodontes cámbricos y *Jujuyaspis keideli* Kobayashi (Trilobita) en el Miembro Alfarcito de la Formación Santa Rosita, quebrada de Humahuaca, Cordillera Oriental de Jujuy: Ameghiniana, v. 46, p. 537–556.

Zeballo, F.J., and Tortello, M.F., 2005, Trilobites del Cámbrico Tardío-Ordovícico Temprano del área de Alfarcito, Tilcara, Cordillera Oriental de Jujuy, Argentina: Ameghiniana, v. 42, p. 127–142.

Zeballo, F.J., Albanesi, G.L., Ortega, G., and Tortello, M.F., 2003, Biostratigraphy of Ordovician sequences from Alfarcito area, Tilcara, Eastern Cordillera of Jujuy, Argentina, *in* Albanesi, G.L., Beresi, M.S., and Peralta, S.H. eds., Ordovician from the Andes: INSUGEO, Serie de Correlación Geológica, v. 17, p. 161–166.

Zeballo, F.J., Albanesi, G.L., and Ortega, G., 2005, Conodontes y graptolitos de las formaciones Alfarcito y Rupasca (Tremadociano) en el área de Alfarcito, Tilcara, Cordillera Oriental de Jujuy, Argentina. Parte 2: Paleontología sistemática: Ameghiniana, v. 42, p. 47–66.

Zeballo, F.J., Albanesi, G.L, and Ortega, G., 2008, New late Tremadocian (Early Ordovician) conodont and graptolite records from the southern South American Gondwana margin (Eastern Cordillera, Argentina): Geologica Acta, v. 6, p. 127–141.

Zeballo, F.J., Albanesi, G.L., and Ortega, G., 2011, Biostratigraphy and paleoenvironments of the Santa Rosita Formation (Late Furongian-Tremadocian), Cordillera Oriental of Jujuy, Argentina, *in* Gutiérrez-Marco, J.C., Rábano, I. and García-Bellido, D. eds., Ordovician of the World: Madrid, Instituto Geológico y Minero de España, Cuadernos del Museo Geominero, v. 14, p. 625–632.

Accepted 25 November 2015